

Translated from: XU C., LIU G., XU G H., et al. The depth and pitch control of submarines based on the pump-hydraulic servo [J]. Chinese Journal of Ship Research, 2017, 12(2): 116-123.

The depth and pitch control of submarines based on the pump-hydraulic servo

XU Chao, LIU Gang, XU Guohua, LI Fengyuan, ZHAI Yunfeng

School of Naval Architecture and Ocean Engineering, Huazhong University of Science and Technology, Wuhan 430074, China

Abstract: This study aims to research submarine motion control features in different conditions and complex environments in order to solve the problem of actual submarine control and apply it to building an actual hydraulic control platform. The paper focuses on the vertical motion of submarines, designs a fast terminal sliding mode control algorithm and analyzes the data using the combined simulation and experiment method to study the robustness and reliability of a submarine's vertical motion control system for hydraulic and control. At the same time, the simulation and experiment results analyze the hysteresis and oscillation of the hydraulic steering gear, and effectively reduce the chattering that may be caused by sliding mode variable structure control. This system can be used in simulations to solve the problems of new submarine control characteristics.

Key words: pump-hydraulic servo; submarine vertical; pitch control; depth control; pitch angle; sliding mode control

CLC number: U664.28

0 Introduction

The control and monitoring of pipeline oil and mechanical mechanism can be realized by designing and building a special platform for the simulation of underwater steering test of submarines, which combines the hydraulic systems of fairwater plane, stern elevator and integrated hydraulic pressure station and is applied to the real submarine structural body. Simulation of submarine's different working conditions and complex environments and establishment of the actual system platform for the experimental research can be used in solving the actual control problem of high-performance submarine.

The traditional hydraulic mechanism mainly contains hydraulic control elements, actuators and loads. The hydraulic servo system mainly uses the incompressibility of liquid and the controllability of flow and direction to control the servo. Hydraulic servo mainly consists of servo valve, variable pump, fuel tank, servo hydraulic cylinder, steering gear and

rudder blade^[1], which uses the variable pump as the hydraulic control element, and shifting fork type steering gear as the actuator, and it combines with the hydrodynamic load of servo to design the pump-hydraulic servo system.

The submarine's steering control is divided into course control on the horizontal plane as well as the depth and pitch control on the vertical plane. Control on the vertical plane is a nonlinear strong coupling multi-input multi-output system. The two pairs of fairwater plane and stern elevator affect the variation of depth and pitch simultaneously, causing interference between the 2 channels of depth and pitch. Generally, the multi-input multi-output system of submarines is converted into single-input single-output system using the decoupling control method^[2], in which the fairwater plane mainly controls the depth, stern elevator main controls the pitch, and the sliding mode control algorithms are designed respectively to realize the control of pitch and depth of submarine.

Received: 2016 - 09 - 06

Author(s): XU Chao, male, born in 1989, master candidate. Research interest: operation technique of underwater robot. E-mail: xuchao20080411@126.com

LIU Gang (Corresponding author), male, born in 1991, Ph.D. candidate. Research interest: operation technique of underwater robot. E-mail: 735877205@qq.com

The control system realized the vertical motion control of submarine based on the pump-hydraulic servo system. Two automatic control algorithms of terminal sliding mode are designed based on the space motion model. Hardware circuit controller and LABVIEW are selected as the display and control of upper computer. Data acquisition of the sensor and algorithm operation are realized in different rudder speeds, and closed-loop control of rudder angle is realized, thus realizing the control of submarine depth and pitch.

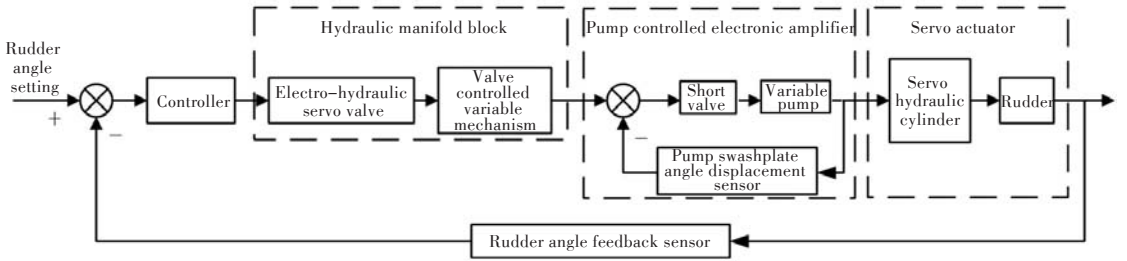


Fig.1 Schematic of hydraulic servo system

The system not only can realize the free switch of pump controlled hydraulic circuit and valve controlled hydraulic circuit, but also has the function of replacing Rexroth pump with the Beijing pump made in China. It uses the Moog proportional valve, Rexroth pump control device and Vickers solenoid valve as the important hydraulic components. The Rexroth electronic amplifier is used to realize the closed cycle of hydraulic servo circuit.

1.1 Main parts of the servo system

Due to the high inherent frequency of hydraulic cylinder load, combined with the closed-loop function of variable pump, Moog electro-hydraulic servo valve of model D660 and its solenoid switch valve are used to compose the hydraulic manifold block. The servo valve model is^[4]

$$G_{sv} = \frac{1/A}{s[\frac{s^2}{W_v^2} + \frac{2\zeta_v}{W_v}s + 1]} \quad (1)$$

Where A is the cross sectional area of servo valve port; s is the Laplace variable of transfer function; ζ_v is the viscosity coefficient of hydraulic oil; and W_v is flow gain.

The Rexroth pump-controlled device with closed loop is used, and the device is composed of a short valve that controls the start and stop of the pump, an A4VSG electronic amplifier that controls the swashplate angle and an axial piston variable pump. The variable pump model is^[5]

$$W_p = n_p K_p \quad (2)$$

Where n_p is the rotational speed of the variable pump; K_p is displacement gradient of the variable pump.

The hydraulic servo actuator is composed of servo hydraulic cylinder and rudder blade. Under the condition of neglecting external force load, the actuator model of the hydraulic cylinder is^[6]

$$W_g = \frac{1/A_g}{s[\frac{s^2}{W_h^2} + \frac{2\zeta_h}{W_h}s + 1]} \quad (3)$$

Where A_g is the effective area of the hydraulic cylinder piston; ζ_h is the hydraulic damping ratio of the hydraulic cylinder; W_h is the natural frequency of the hydraulic cylinder.

In the system, 8 rudder angle feedback sensors with adjustable gain are selected respectively for the fairwater plane and the stern elevator, and the filtering algorithm is used to realize the multi-directional and accurate measurement of the rudder angle, completing the upper computer display of the rudder angle and the algorithm operation.

1.2 AMESIM model of servo system

The hydraulic system model is established by combining the component parameters of the real pump-hydraulic servo system. The characteristics of the hydraulic system are studied by AMESIM simulation, and the schematic of the simulation is shown in Fig. 2

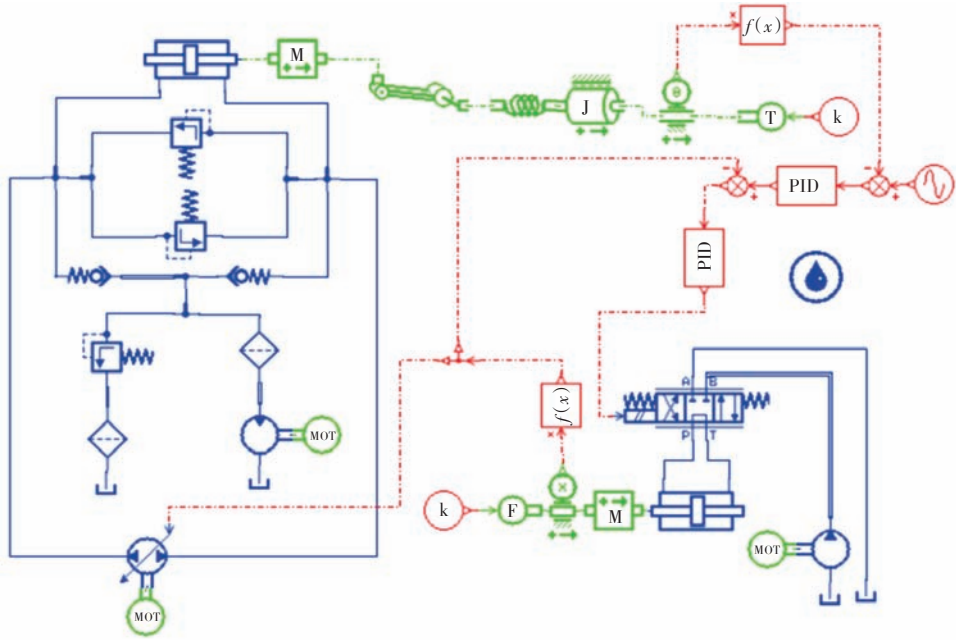


Fig.2 AMESIM schematic of hydraulic servo system

The tracking stability of rudder angle is studied under the setting of the rudder angle of the sinusoidal signal (Fig. 3). In Fig. 3, the tracking characteristics of hydraulic servo system are researched using AMESIM simulation. The maximum deviation of setting rudder angle and feedback rudder angle is calculated. We obtained that the maximum overshoot is

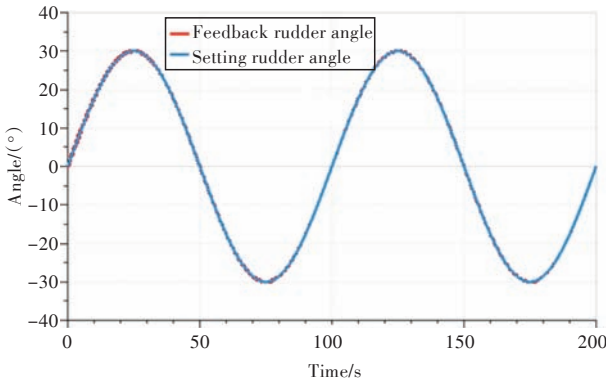


Fig.3 The tracking curve of rudder angle

2.1%, the rudder angle tracking time is about 3.2 s/(°), and stable tracking time at 30° hard-over angle is about 120 s (rudder speed of 4 s/(°)). The system parameter performance meets the test requirements.

1.3 Nonlinear model for vertical motion of submarine

Ignoring the influence of horizontal motion, the spatial six degrees of freedom (DOF) motion equation of submarine is simplified, and the vertical motion model is obtained. The strong nonlinearity and strong coupling of submarine depth and pitch control are studied^[7]. According to the spatial six DOF standard motion equation of United States Naval Ship (USNS) research, the following vertical motion equation can be obtained without considering the horizontal motion state and the nonlinear term of the system:

$$\begin{cases}
 (m - \frac{1}{2}\rho L^3 X_u^{\prime})\dot{u} = \frac{1}{2}\rho L^4 (X_{qq}^{\prime} q^2) + \frac{1}{2}\rho L^2 (a_T u^2 + b_T u u_c + c_T u_c^2) + \frac{1}{2}\rho L^2 (X_{uu}^{\prime} u^2 + X_{ww}^{\prime} w^2 + X_{\delta_s \delta_s}^{\prime} u^2 \delta_s^2 + X_{\delta_s \delta_b}^{\prime} u^2 \delta_b^2) + \\
 \quad \frac{1}{2}\rho L^3 (X_{wq}^{\prime} wq - m^{\prime} wq) \\
 m(\dot{w} - uq) = \frac{1}{2}\rho L^4 (Z_q^{\prime} \dot{q} + Z_{q|q}^{\prime} q|q|) + \frac{1}{2}\rho L^3 (Z_w^{\prime} \dot{w} + Z_q^{\prime} uq + Z_{w|q}^{\prime} w|q| + Z_{|q|\delta_s}^{\prime} u|q|\delta_s) + \\
 \quad \frac{1}{2}\rho L^2 (Z_{uu}^{\prime} u^2 + Z_w^{\prime} uw + Z_{|w|}^{\prime} u|w| + Z_{w|w|}^{\prime} w|w| + Z_{ww}^{\prime} w^2) + \frac{1}{2}\rho L^2 (Z_{\delta_s}^{\prime} u^2 \delta_s + Z_{\delta_b}^{\prime} u^2 \delta_b) + P \\
 I_y \dot{q} = \frac{1}{2}\rho L^5 (M_q^{\prime} \dot{q} + M_{q|q}^{\prime} q|q|) + \frac{1}{2}\rho L^4 (M_w^{\prime} \dot{w} + M_q^{\prime} uq + M_{w|q}^{\prime} w|q| + M_{|q|\delta_s}^{\prime} u|q|\delta_s) + \\
 \quad \frac{1}{2}\rho L^3 (M_{uu}^{\prime} u^2 + M_w^{\prime} uw + M_{|w|}^{\prime} u|w| + M_{w|w|}^{\prime} w|w| + M_{ww}^{\prime} w^2) + \frac{1}{2}\rho L^3 (M_{\delta_s}^{\prime} u^2 \delta_s + M_{\delta_b}^{\prime} u^2 \delta_b) + MP \\
 \theta = q \\
 \dot{\zeta} = w \cos \theta - u \sin \theta
 \end{cases} \quad (4)$$

Where m is the submarine mass; ρ is seawater density; L is the submarine length; X is the longitudinal force; Z is the vertical force; M is the pitch moment; a_T, b_T, c_T are velocity coefficients; P is static load; δ_b is rudder angle of fairwater plane; δ_s is rudder angle of stern elevator; u, w, θ, q are the longitudinal velocity, vertical velocity, pitch angle and pitch angle velocity of submarine, respectively; $\dot{u}, \dot{w}, \dot{q}$ are the longitudinal accelera-

$$\begin{cases} \dot{w} = \frac{k_{3q}f_2 - k_{2q}f_3}{k_{2w}k_{3q} - k_{2q}k_{3w}} + \frac{k_{3q}b_{2s} - k_{2q}b_{3s}}{k_{2w}k_{3q} - k_{2q}k_{3w}}\delta_s + \frac{k_{3q}b_{2b} - k_{2q}b_{3b}}{k_{2w}k_{3q} - k_{2q}k_{3w}}\delta_b = f_w + b_{ws}\delta_s + b_{wb}\delta_b \\ \dot{q} = \frac{-k_{3w}f_2 + k_{2w}f_3}{k_{2w}k_{3q} - k_{2q}k_{3w}} + \frac{-k_{3w}b_{2s} + k_{2w}b_{3s}}{k_{2w}k_{3q} - k_{2q}k_{3w}}\delta_s + \frac{-k_{3w}b_{2b} + k_{2w}b_{3b}}{k_{2w}k_{3q} - k_{2q}k_{3w}}\delta_b = f_q + b_{qs}\delta_s + b_{qb}\delta_b \\ \dot{\theta} = q \\ \dot{\zeta} = w \cos \theta - u \sin \theta \end{cases} \quad (5)$$

Where k, f and b are the simplified variables of parameters in Eqs. (4)-(5);

$$\begin{aligned} f_w &= \frac{k_{3q}f_2 - k_{2q}f_3}{k_{2w}k_{3q} - k_{2q}k_{3w}}, & b_{ws} &= \frac{k_{3q}b_{2s} - k_{2q}b_{3s}}{k_{2w}k_{3q} - k_{2q}k_{3w}}, & b_{wb} &= \frac{k_{3q}b_{2b} - k_{2q}b_{3b}}{k_{2w}k_{3q} - k_{2q}k_{3w}}, \\ f_q &= \frac{-k_{3w}f_2 + k_{2w}f_3}{k_{2w}k_{3q} - k_{2q}k_{3w}}, & b_{qs} &= \frac{-k_{3w}b_{2s} + k_{2w}b_{3s}}{k_{2w}k_{3q} - k_{2q}k_{3w}}, & b_{qb} &= \frac{-k_{3w}b_{2b} + k_{2w}b_{3b}}{k_{2w}k_{3q} - k_{2q}k_{3w}}. \end{aligned}$$

The initial state is set: vertical velocity $v=0$, roll angle velocity $p=0$, pitch angle velocity $r=0$, yaw angle $\psi=0$, the lateral acceleration of hull $\dot{v}=0$, roll angle acceleration $\dot{p}=0$, and yaw angle acceleration $\dot{\psi}=0$.

2 Controller design

The terminal sliding mode control algorithm is adopted in this paper. Terminal sliding mode variable structure control algorithm has strong robustness to parameter perturbation and external disturbance satisfying the matching conditions. The algorithm designs the sliding mode surface based on the nonlinear model, so that the terminal sliding mode control theory features with good performance of finite time convergence and fast omnidistance convergence^[8], which can adapt to the control model of strong nonlinearity and coupling on the vertical plane of submarine.

2.1 Principle of sliding mode variable structure

For the nonlinear systems, the "structure" of sliding mode variable structure control is not fixed due to the discontinuity of control function, and the change law depends on the current state of the sys-

tem, vertical acceleration and pitch angle acceleration of submarine, respectively; u_c is velocity component in the axial force direction; I_y is moment of inertia of axis y ; and $\dot{\zeta}$ is the change rate of depth.

The variation of vertical velocity, pitch angle velocity, pitch angle and depth value should be measured in the model. The variables in Eq. (4) are solved to simplify the model, and there is

tem in the dynamic process

$$\dot{x} = f(x, u, t); \quad x \in \mathbf{R}^n, \quad u \in \mathbf{R}^m, \quad t \in \mathbf{R} \quad (6)$$

Where u is input quantity and x is system variable.

Sliding mode variable structure design needs to first determine the switching function $S(x), S \in \mathbf{R}^m$ so as to ensure that the sliding mode control has steady-state characteristics. The dimension of this function determines the dimension of the control, and the function vector has the sliding mode field and the characteristics of asymptotic stability of sliding motion^[9] (Fig. 4).

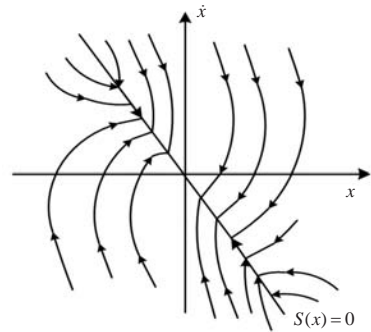


Fig.4 Asymptotic stability schematic of sliding mode motion

Then, variable structure control is sought:

$$u(x, t) \in \begin{cases} u^+(x), S(x) > 0 \\ u^-(x), S(x) < 0 \end{cases} \quad (7)$$

$u^+(x) \neq u^-(x)$ reflects the characteristics of variable structure, as shown in Fig. 5.

The specific steps of the steady-state sliding mode algorithm are summarized as follows (Fig. 6):

1) Design of sliding mode variable structure $u(x)$: if $S(x) < 0$, then $\dot{S} > 0$; if $S(x) > 0$, then $\dot{S} < 0$, which makes the points out of the sliding mode surface $S(x)=0$ in the system reach the sliding mode

surface in finite time (reachability condition), thus the system enters the sliding mode field (existence condition).

2) Design of the sliding mode surface switching function $S(x)$: when the system reaches the sliding mode surface, it gradually arrives at the origin along the switching function, so that the system has stable control effect (stability condition).

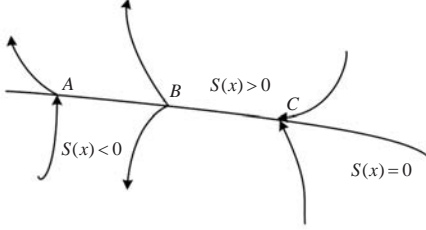


Fig. 5 Variable structure schematic of sliding mode control method

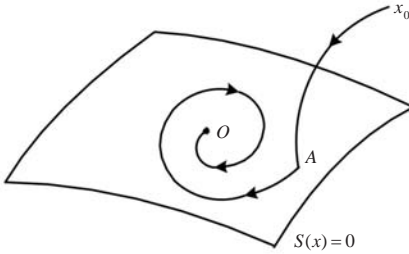


Fig. 6 The steady process schematic of sliding mode control method

2.2 Design of sliding mode variable structure controller

2.2.1 Sliding mode reaching law and sliding mode surface design

At a certain speed, combined with the performance of the fairwater plane and the stern elevator, the submarine can reach the specified depth from the initial depth, and the control requirements of pitch angle are realized in the meantime. Neglecting the coupling effects of the fairwater plane and the stern elevator, the independent sliding mode control algorithms are designed to overcome the errors caused by the coupling effect.

The second order nonlinear system is as follows:

$$\begin{cases} \dot{x}_1 = x_2 \\ x_2 = f(x) + g(x)u + d(t) \end{cases} \quad (8)$$

Where $x = [x_1, x_2]$, in which x_1 and x_2 are system variables; $f(x)$ and $g(x)$ are smooth functions, and $g(x) \neq 0$; $d(t)$ is a disturbance term.

The fast terminal sliding mode surface is designed as follows:

$$s_1 = \dot{s}_0 + \alpha_0 s_0 + \beta_0 s_0^{q_0/p_0} \quad (9)$$

Where $\alpha_0, \beta_0 > 0$; $q_0, p_0 (q_0 < p_0)$ are positive odd numbers; $s_0 = x_1$; the linear term $\alpha_0 s_0$ is fast reaching surface; the nonlinear term $\beta_0 s_0^{q_0/p_0}$ can ensure that the system moves to the sliding mode surface within the required time.

In addition, the reaching law enables the system to have good dynamic quality in the neighboring regions, and the fast terminal reaching law can be designed as follows^[10]:

$$\dot{s}_1 = -\phi s_1 - \gamma s_1^{q/p} + d(t) \quad (10)$$

Where $\gamma, \phi > 0$; $p, q (q < p)$ are positive odd numbers; $d(t)$ is external disturbance, and $|d(t)| \leq L$. The fast terminal sliding mode reaching law, which uses positive and negative signs for switching, is used to replace the sign function so that the system can rapidly reach the sliding mode surface $s(t)=0$ from the initial state in a limited time. Moreover, compared with the general reaching law, this reaching law can reduce the chattering caused by the sign function in discontinuous region. By Formula (9), there is

$$\begin{aligned} \dot{s}_1 = \dot{s}_0 + \alpha_0 \dot{s}_0 + \beta_0 \frac{d}{dt} s_0^{p_0} = \\ f(x) + g(x)u + \alpha_0 \dot{s}_0 + \beta_0 \frac{d}{dt} s_0^{p_0} \end{aligned} \quad (11)$$

According to Eqs. (10) and (11), the fast terminal sliding mode controller can be optimized as

$$u(t) = -g(x)^{-1} \left[f(x) + \alpha_0 \dot{s}_0 + \beta_0 \frac{d}{dt} s_0^{p_0} + \phi s_1 + \gamma s_1^{q/p} \right] \quad (12)$$

According to the Lyapunov function, there is $V = \frac{1}{2} s_1^2$. The derivative is taken as follows:

$$\dot{V} = s_1 \dot{s}_1 = -\phi s_1^2 - \gamma s_1^{(p+q)/p} + s_1 d(t) \quad (13)$$

Where $(p+q)$ is even number, then $\dot{V} = -\phi s_1^2 - \gamma s_1^{(p+q)/p} + s_1 d(t) \leq 0$, that is $\gamma \geq \left| \frac{1}{s_1^{q/p}} \right| L$.

2.2.2 Sliding mode reaching law on vertical plane and design of sliding mode surface

In order to realize depth and pitch control on the vertical plane of submarine, two kinds of automatic control algorithms are designed based on the vertical motion model of submarine, and the experiment and simulation analysis are carried out.

Depth deviation is set to $e_s = \zeta - \zeta_d$, and pitch angle deviation $e_\theta = \theta - \theta_d$, namely, the change rate $\dot{e}_s = \dot{\zeta} - \dot{\zeta}_d$, $\dot{e}_\theta = \dot{\theta} - \dot{\theta}_d$. The fast terminal sliding mode surfaces for submarine depth and pitch control are designed respectively:

$$\begin{cases} \dot{s}_s = k_{1s}e_s + k_{2s}|e_s|^{l_s} \text{sign}(e_s) + \dot{e}_s \\ \dot{s}_\theta = k_{1\theta}e_\theta + k_{2\theta}|e_\theta|^{l_\theta} \text{sign}(e_\theta) + \dot{e}_\theta \end{cases} \quad (14)$$

Where partial parameter perturbation can be satisfied when parameters $k_{1s}, k_{2s}, k_{1\theta}, k_{2\theta}$ are designed; $0 < l_s < 1; \quad 0 < l_\theta < 1$. Let $f(x) = k_{1s}e_s + k_{2s}|e_s|^{l_s} \text{sign}(e_s)$ and $f(x) = k_{1\theta}e_\theta + k_{2\theta}|e_\theta|^{l_\theta} \text{sign}(e_\theta)$. According to the terminal sliding mode control characteristic, once the system enters the sliding mode surface, the depth and pitch errors will reach zero point within a certain time.

$$\begin{aligned} \dot{s}_s &= k_{1s}\dot{e}_s + k_{2s}l_s|e_s|^{l_s-1} \text{sign}(e_s)\dot{e}_s + \ddot{e}_s = \\ & \dot{w} \cos \theta - wq \sin \theta - uq \cos \theta - \dot{u} \sin \theta - \\ & \dot{\zeta}_d + k_{1s}\dot{e}_s + k_{2s}l_s|e_s|^{l_s-1} \text{sign}(e_s)\dot{e}_s = \\ & (f_w + g_w \delta_s) \cos \theta - wq \sin \theta - uq \cos \theta - \dot{u} \sin \theta - \\ & \dot{\zeta}_d + k_{1s}\dot{e}_s + k_{2s}l_s|e_s|^{l_s-1} \text{sign}(e_s)\dot{e}_s = \\ & \cos \theta (g_w \delta_s + f_w + f_s) \end{aligned} \quad (15)$$

$$\begin{aligned} \dot{s}_\theta &= k_{1\theta}\dot{e}_\theta + k_{2\theta}l_\theta|e_\theta|^{l_\theta-1} \text{sign}(e_\theta)\dot{e}_\theta + \ddot{e}_\theta = \\ & -\dot{\theta}_d + k_{1\theta}\dot{e}_\theta + k_{2\theta}l_\theta|e_\theta|^{l_\theta-1} \text{sign}(e_\theta)\dot{e}_\theta = \\ & f_q + b_{qs}\delta_s + b_{qb}\delta_b - \dot{\theta}_d + k_{1\theta}\dot{e}_\theta + \\ & k_{2\theta}l_\theta|e_\theta|^{l_\theta-1} \text{sign}(e_\theta)\dot{e}_\theta \end{aligned} \quad (16)$$

Where $f_s = \frac{1}{\cos \theta} [-wq \sin \theta - uq \cos \theta - \dot{u} \sin \theta - \dot{\zeta}_d + k_{1s}\dot{e}_s + k_{2s}l_s|e_s|^{l_s-1} \text{sign}(e_s)\dot{e}_s]$. The automatic control algorithms for submarine depth and pitch are designed by using the fast terminal reaching law:

$$\begin{cases} \dot{s}_s = -k_{3s}s_s - k_{4s}(|s_s|^{l_{3s}} + |s_s|^{l_{2s}}) \text{sign}(s_s) = ds_s \\ \dot{s}_\theta = -k_{3\theta}s_\theta - k_{4\theta}(|s_\theta|^{l_{3\theta}} + |s_\theta|^{l_{2\theta}}) \text{sign}(s_\theta) = ds_\theta \end{cases} \quad (17)$$

Combined with Eqs. (15)–(17), the governing equations of the rudder angle δ_s of fairwater plane and the rudder angle δ_b of stern elevator are obtained:

$$\begin{cases} \dot{\delta}_s = (\frac{ds_s}{\cos \theta} - f_w - g_w \delta_s - f_s) / b_{wb} \\ \dot{\delta}_b = (ds_\theta - f_q - b_{qs} \delta_s + \dot{\theta}_d - k_{1\theta} \dot{e}_\theta - \\ k_{2\theta} l_\theta |e_\theta|^{l_\theta-1} \text{sign}(e_\theta) \dot{e}_\theta) / b_{qb} \end{cases} \quad (18)$$

The Lyapunov function of Eq. (17) is:

$$\begin{cases} V_1 = \frac{1}{2} s_s^2 \\ V_2 = \frac{1}{2} s_\theta^2 \end{cases} \quad (19)$$

Then $V_1 \dot{V}_1 = s_s \dot{s}_s = -k_{3s} s_s - k_{4s} (|s_s|^{l_{3s}} + |s_s|^{l_{2s}}) \text{sign}(s_s) \leq 0$, $V_2 \dot{V}_2 = s_\theta \dot{s}_\theta = -k_{3\theta} s_\theta - k_{4\theta} (|s_\theta|^{l_{3\theta}} + |s_\theta|^{l_{2\theta}}) \text{sign}(s_\theta) \leq 0$. Therefore, the sliding mode control of submarine depth and pitch has the system stability.

3 Simulation and test

3.1 Simulation results

Combined with the AMESIM model pump-hydraulic servo and the Matlab model for vertical motion of submarines, the design principle of decoupling controller is used to design terminal sliding mode controller and control the fairwater plane and stern elevator affecting the depth and pitch. The co-simulation of Simulink and AMESIM is conducted (Fig. 7), so that the submarine arrived at the specified depth in limited time, and control of pitch angle is completed. The simulation results show that the terminal sliding mode control algorithm can well adapt to the strong nonlinearity and coupling on the vertical plane of submarine^[11], indicating that the control system can effectively reduce the chattering of sliding mode variable structure.

It is assumed that the submarine's longitudinal propulsion velocity is good; displacement of the submarine $\nabla_\downarrow = 1500 \text{ m}^3$; seawater density $\rho = 1.025 \times 10^3 \text{ kg/m}^3$; length of the submarine $L = 70 \text{ m}$; the submarine's height and width $H = B = 6 \text{ m}$; velocity $u = 6 \text{ kn}$. The parameters of fast terminal sliding

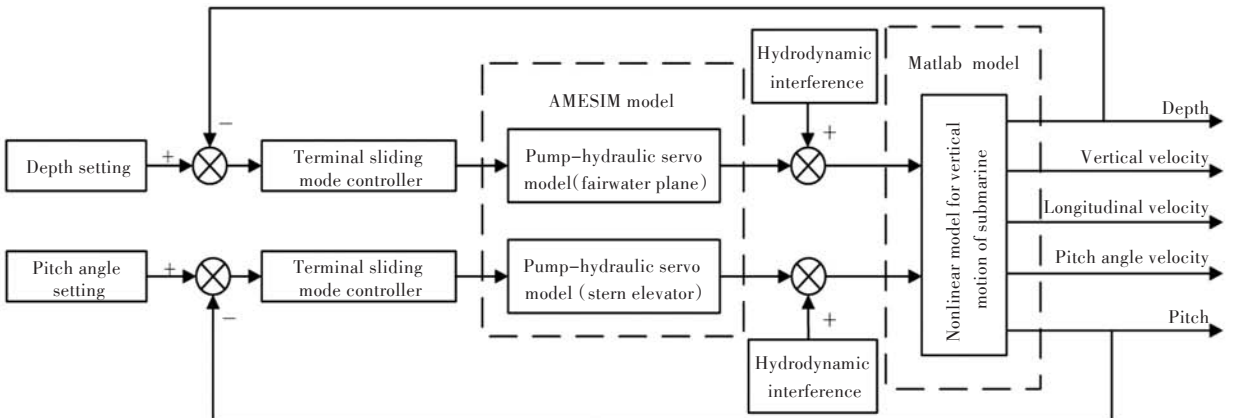


Fig. 7. The system schematic of co-simulation

mode controller are: $k_{1s}=0.5$, $k_{2s}=0.001$, and $l_s=1.6$. The parameters of fast terminal sliding mode reaching law are: $k_{3s}=0.3$, $k_{4s}=0.005$, $l_{1s}=0.8$, and $l_{2s}=2.3$.

1) The depth and pitch tracking characteristics are studied for sinusoidal signal input, and the simulation results are shown in Figs. 8–9.

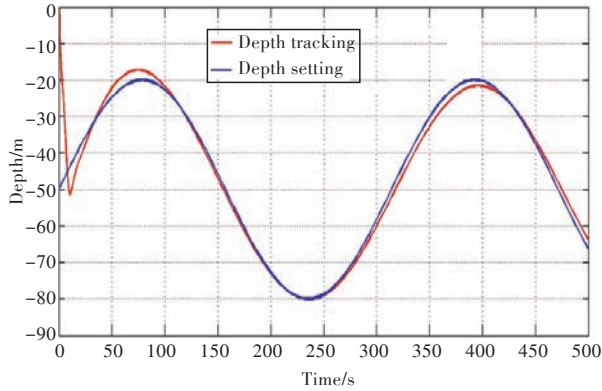


Fig.8 The depth tracking curve for sinusoidal signal input

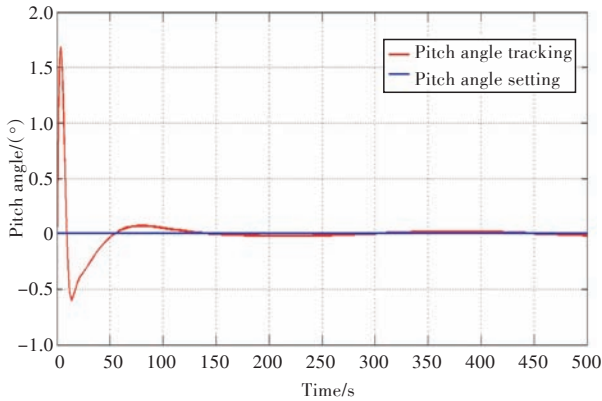


Fig.9 Pitch angle tracking curve for sinusoidal signal input

2) The depth and pitch tracking characteristics are studied for Sigmoid signal input, and the simulation results are shown in Figs. 10–11.

Due to the uncertainties, errors and variability of the external disturbances in the calculation of submarine parameters, the predictive model has some deviations from the real submarine model in the process

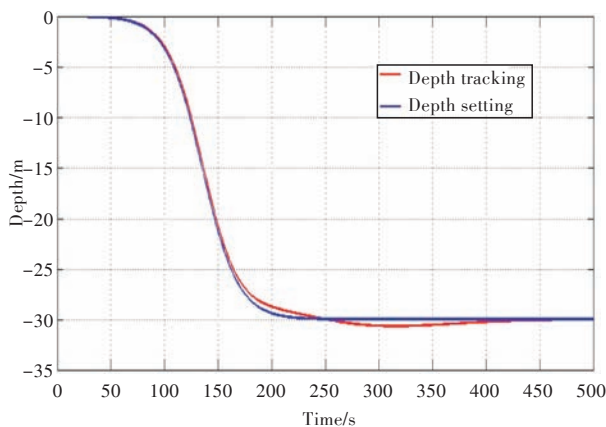


Fig.10 The depth tracking curve for Sigmoid signal input

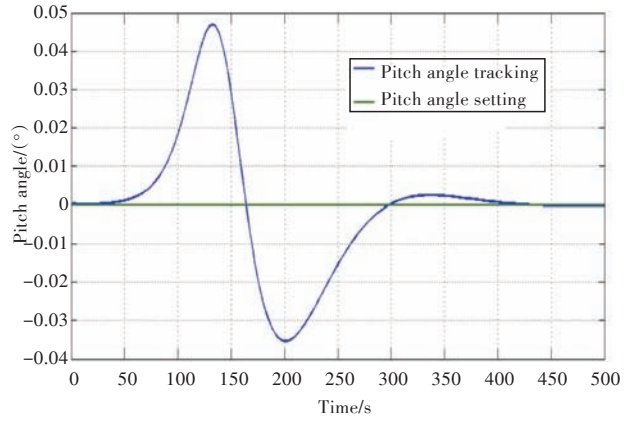


Fig.11 Pitch angle tracking curve for Sigmoid signal input

of system control. Using the parameter perturbation method, assuming that system model is changed, this paper uses the same control algorithms for research. The two simulation results are compared so as to research the robustness of the control algorithm and the adaptability to the external disturbance before and after the model change, thus to verify that the model still has reliability and stability in the system control under some changes.

1) The model's response curves of parameter perturbation for sinusoidal signal input are shown in Figs. 12–13.

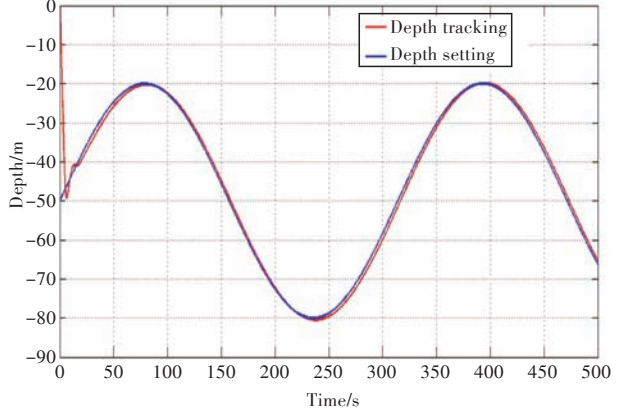


Fig.12 The depth tracking curve for sinusoidal signal input and parameter perturbation

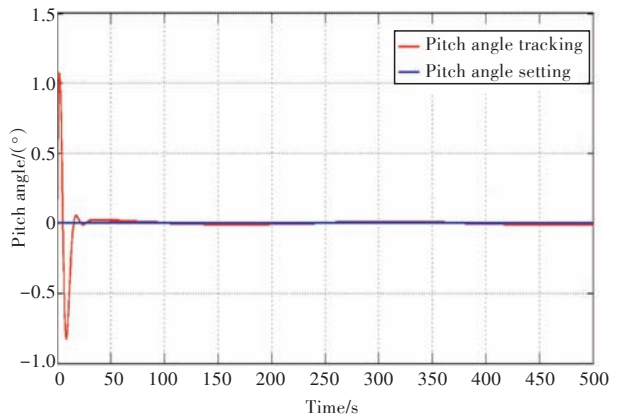


Fig.13 Pitch angle tracking curve for sinusoidal signal input and parameter perturbation

2) The model's response curves of parameter perturbation for Sigmoid signal input are shown in Figs. 14–15.

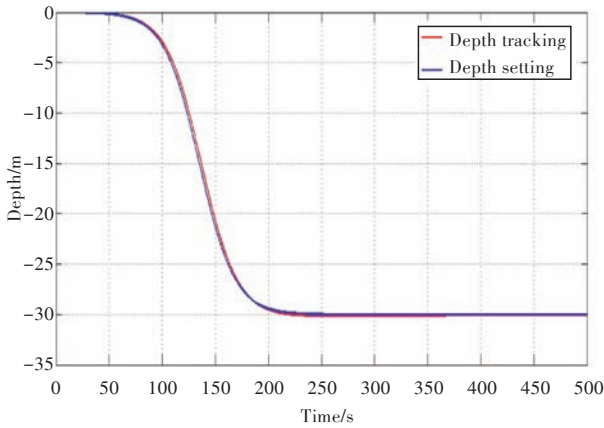


Fig. 14 The depth tracking curve for Sigmoid signal input and parameter perturbation

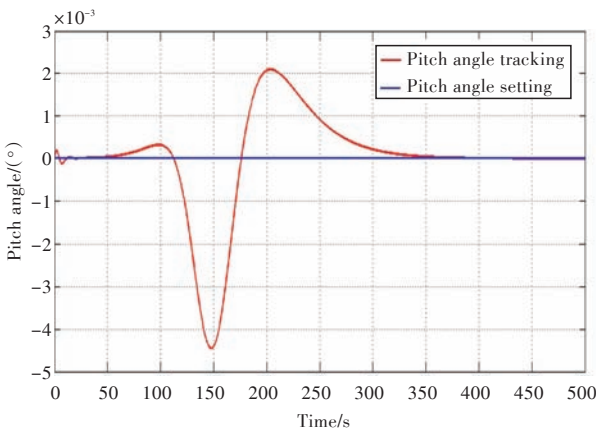


Fig. 15 Pitch angle tracking curve for Sigmoid signal input and parameter perturbation

3.2 System test

The system not only conducts the research of full digital simulation, but also completes the semi-physical system test, which can simulate submarine control in a variety of complex conditions, realizing the dual mode operation of local and remote control of submarine, as well as simulation tests at full rudder speed and half rudder speed. For the signal acquisition of analog quantity such as sensor participating in closed-loop control and the pump-controlled swashplate angle, the filtering algorithm is used in the test to ensure the accuracy and validity of signal. Combined with the hydraulic impact that nonlinear algorithm may produce on the hydraulic system, the design and test of power principle of the total system are completed.

The semi-physical simulation platform is used for the system test joint debugging. A semi-physical model was built (Figs. 16–18), and the simulation of

the actuator and the control object was carried out. Finally, the actual control system connection as well as function and performance debugging was conducted. The controller on-line monitoring curve displays the control effect of setting, tracking and feedback in real-time (Fig. 19). The green curve is the setting value; the red curve is the controller output value; and the blue curve is the sensor feedback value.

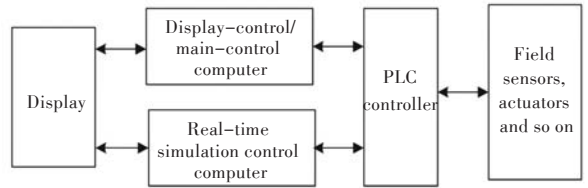


Fig. 16 The structure schematic of system experiment



Fig. 17 The image of system experiment



Fig. 18 The image of semi-physical simulation system

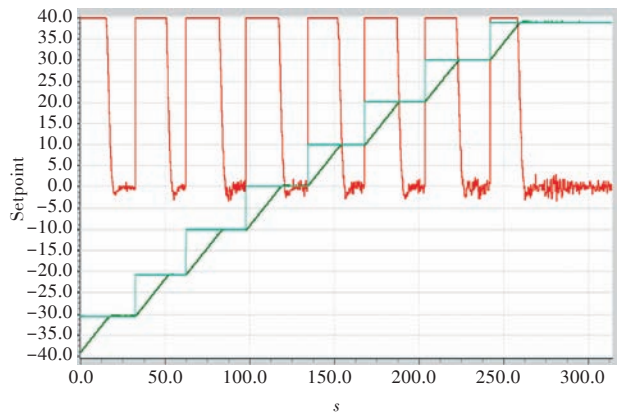


Fig. 19 The effect curves of practical experiment

4 Conclusion

In this paper, a simplified spatial six DOF equation is established, and the vertical motion model of submarine is obtained. In order to control the vertical depth and pitch angle control of submarines, the controller is designed respectively to make the submarine reach a steady setting depth in a limited time and the control of pitch angle completed at the same time. The controller can effectively reduce the chattering of sliding mode variable structure control. The co-simulation of AMESIM and Matlab is used in this paper to analyze the stability and reliability of the system, and the actual project testing is carried out. The research results not only validate the good vertical control performance of this control method in theory, but also verify that the system has good robustness and reliability in the test state, which is in line with the modern submarine demand.

References

- [1] LIU H Y, LIANG L H, ZHANG L Y. Submarine hydraulic steering gear fuzzy logic control method [J]. Journal of Sichuan Ordnance, 2006, 33(11): 93-96 (in Chinese).
- [2] XIA J, HU D B. Research of depth control of submarine based on terminal sliding control [J]. Ship Science and Technology, 2012, 34(2): 55-58, 62 (in Chinese).
- [3] PENG L K, YE F, XING J F. Characteristic analysis of pressure shock of the hydraulic cylinder for pump-controlled steering system [J]. Ship Science and Technology, 2013, 35(9): 74-79 (in Chinese).
- [4] YU W B, LI D Y, HUANG Y N, et al. Analysis of mathematical model of hydraulic servo system of submarine steering gear [J]. Ship Engineering, 2002(4): 38-42 (in Chinese).
- [5] TONG S G, WANG X B, ZHONG W, et al. Dynamic characteristics analysis on axial piston pump based on virtual prototype technology [J]. Journal of Mechanical Engineering, 2013, 49(2): 174-182 (in Chinese).
- [6] JI T. Modeling and simulation of hydraulic system for ship steering gear [D]. Dalian: Dalian Maritime University, 2013: 31-35 (in Chinese).
- [7] SHI S D. Maneuverability of submarine [M]. Beijing: National Defense Industry Press, 1995 (in Chinese).
- [8] SU Z X. Attitude and position control algorithms based on terminal sliding theory research for satellite [D]. Harbin: Harbin Institute of Technology, 2012: 17-20 (in Chinese).
- [9] KANG Y. The study and application of variable structure control theory [D]. Hefei: Hefei University of Technology, 2002: 8-10 (in Chinese).
- [10] LIU G, XU G H, CHEN Y, et al. A novel terminal sliding mode control for the navigation of an under-actuated UUV [C]//The 26th International Ocean and Polar Engineering Conference. Rhodes, Greece: International Society of Offshore and Polar Engineers, 2016.
- [11] MOU J, ZHOU C X, XU H Z. Sliding mode controlling of submarine vertical movement [J]. Ship Science and Technology, 1997(2): 1-5 (in Chinese).

基于泵控液压舵机的潜艇深度及纵倾控制

徐超, 刘刚, 徐国华, 李逢园, 翟云峰

华中科技大学 船舶与海洋工程学院, 湖北 武汉 430074

摘要: [目的] 针对不同工况、复杂环境下的潜艇运动控制进行研究, 解决高性能潜艇的实际控制问题并将其运用于搭建实际液压控制平台。[方法] 以潜艇垂直面运动为重点, 设计垂直面上纵倾和深度模型的解耦控制。基于泵控液压舵机模型和潜艇垂直面运动数学模型, 运用快速终端滑模控制算法, 通过仿真和试验对系统进行分析。[结果] 结合液压系统模型与非线性控制算法的研究论证了该系统在潜艇垂直面运动控制上的鲁棒性与可靠性。与此同时, 对液压舵机滞后、振荡性进行的仿真及试验分析, 也表明系统可有效降低滑模变结构控制带来的抖振问题。[结论] 该系统在模拟研究潜艇的控制特性问题方面具有工程应用价值。

关键词: 泵控液压舵机; 潜艇垂直面; 纵倾控制; 深度控制; 纵倾角; 滑模控制